Electronic Supplementary Information

A pyrene-benzimidazole composed effective fluoride sensor: potential mimicking of a Boolean logic gate

Archana Kushwaha[a], Sagar K. Patil[a] and Dipanwita Das[a,*]

[a]*Department of Chemistry, Institute of Chemical Technology, Matunga, Mumbai 400019 (India)*

Fax: (91)022-3361-1020

E-mail: dr.das@ictmumbai.edu.in

Table S1 Selected bond distances (Å) and bond angles (º) for receptor **2**.

	2
C(4)−C(5)	1.389(2)
C(5)−N(2)	1.374(19)
C(5)−C(6)	1.399(19)
C(6)−N(1)	1.389(18)
C(7)−N(1)	1.326(18)
C(7)–N(2)	1.358(17)
C(7)–C(8)	1.472(2)
C(8)–C(9)	1.394(2)
C(8)–C(21)	1.410(2)
N(2)–H(1B)	0.931(17)
C(6)−C(1)−H(1)	121.0
C(5)−C(4)−H(4)	121.6
N(2)−C(5)−C(4)	132.12(13)
N(2)−C(5)−C(6)	105.58(12)
C(4)−C(5)−C(6)	122.27(14)
C(1)−C(6)−N(1)	130.43(13)
C(1)−C(6)−C(5)	119.99(13)
N(1)−C(6)−C(5)	109.55(12)
N(1)−C(7)−N(2)	112.56(12)
N(1)−C(7)−C(8)	125.57(12)
N(2)−C(7)−C(8)	121.65(13)
C(9)−C(8)−C(21)	119.66(14)
C(9)−C(8)−C(7)	117.51(13)
C(21)−C(8)−C(7)	122.77(13)
C(8)−C(21)−C(20)	123.34(14)
C(7)−N(1)−C(6)	104.99(11)
C(7)−N(2)−C(5)	107.32(12)
C(7)−N(2)−H(1B)	125.9(10)

Table S2. Intermolecular hydrogen bond distances (Å) and bond angles (º) in receptor **2**.

D–H···A	d(D–H)	d(H···A)	D···A	∠(DHA)
N(2)–H(1B)···N(1)	0.931(17)	1.954(18)	2.8638(16)	165.4(15)

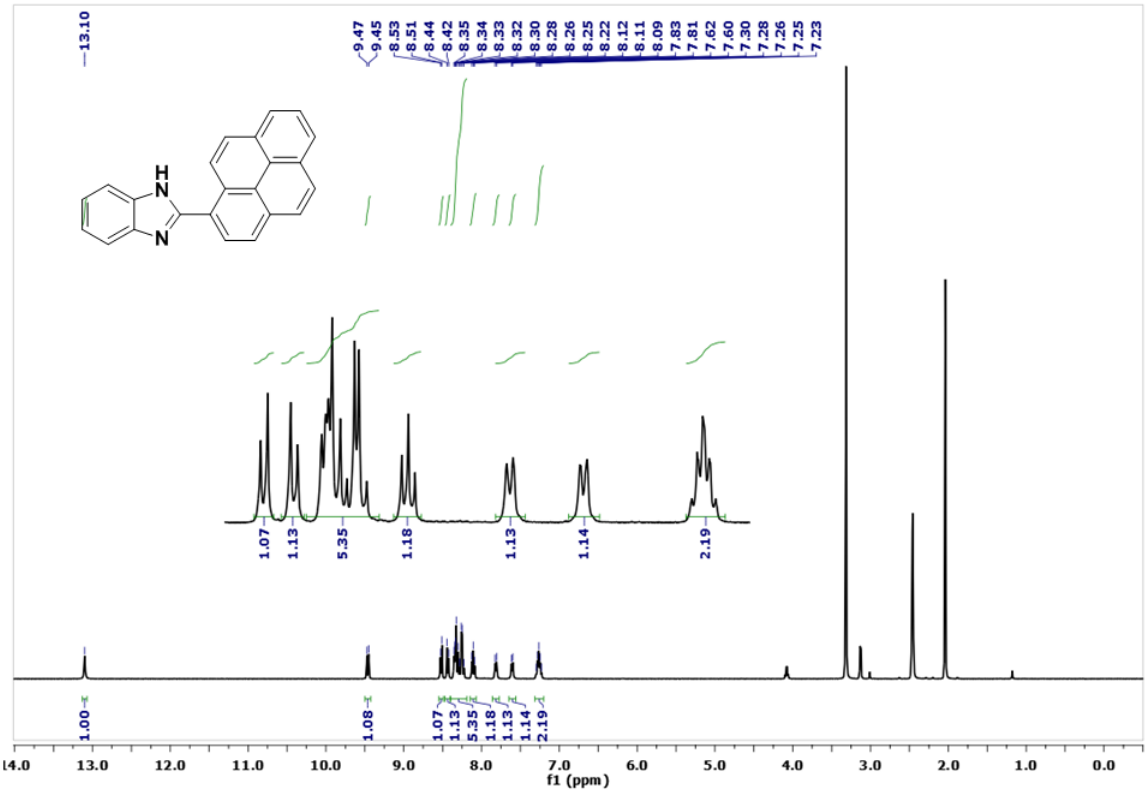

Fig. S1 ^{1}H NMR (400 MHz, DMSO-d_6) spectrum of receptor **2**.

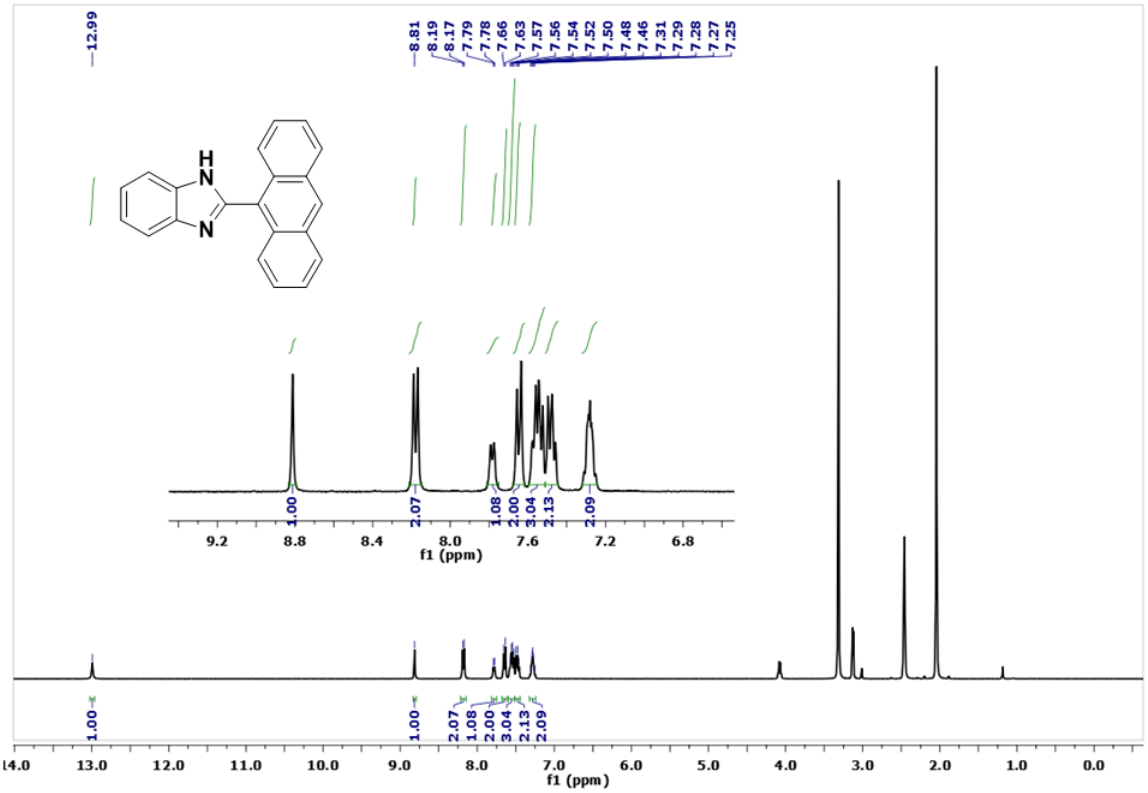

Fig. S2 ^{1}H NMR (400 MHz, DMSO-d_6) spectrum of receptor **3**.

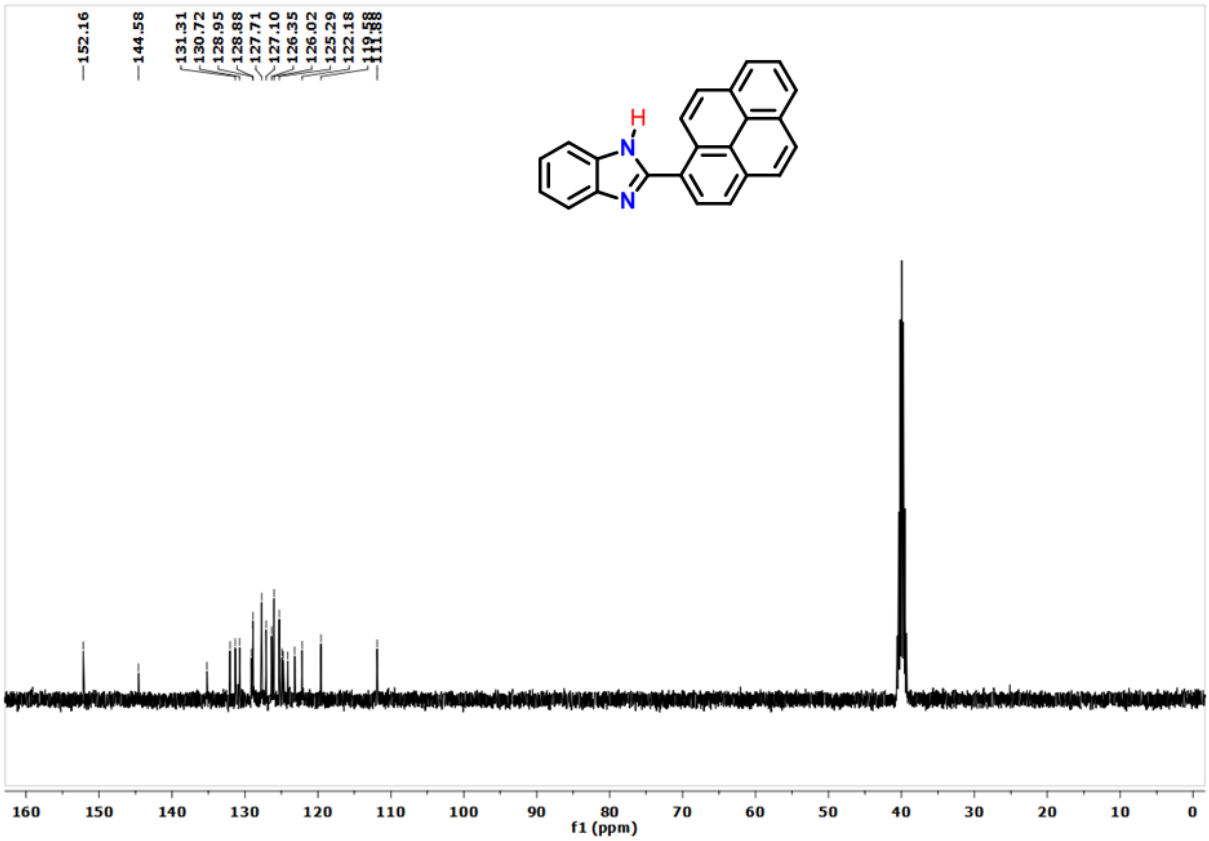

Fig. S3 ^{13}C NMR (101 MHz, DMSO-d_6) spectrum of receptor **2**.

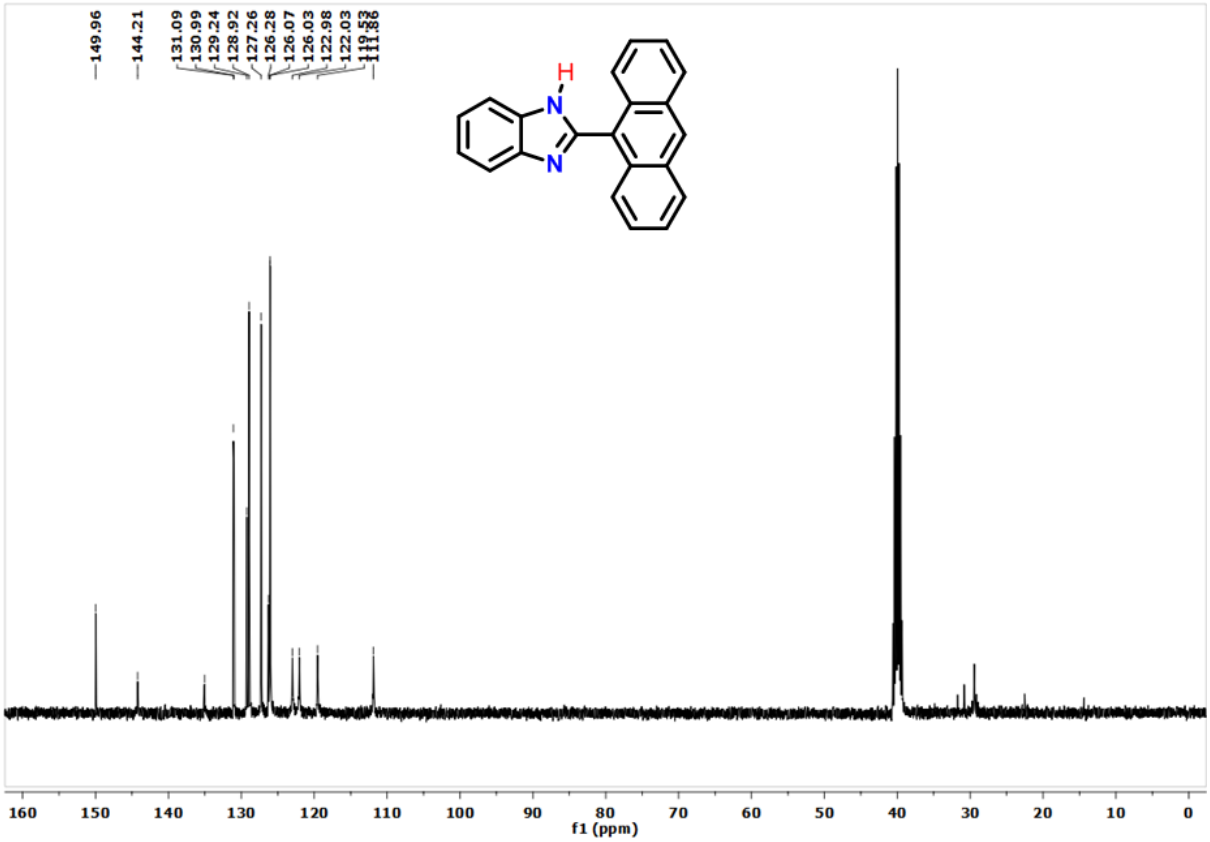

Fig. S4 ^{13}C NMR (101 MHz, DMSO-d_6) spectrum of receptor **3**.

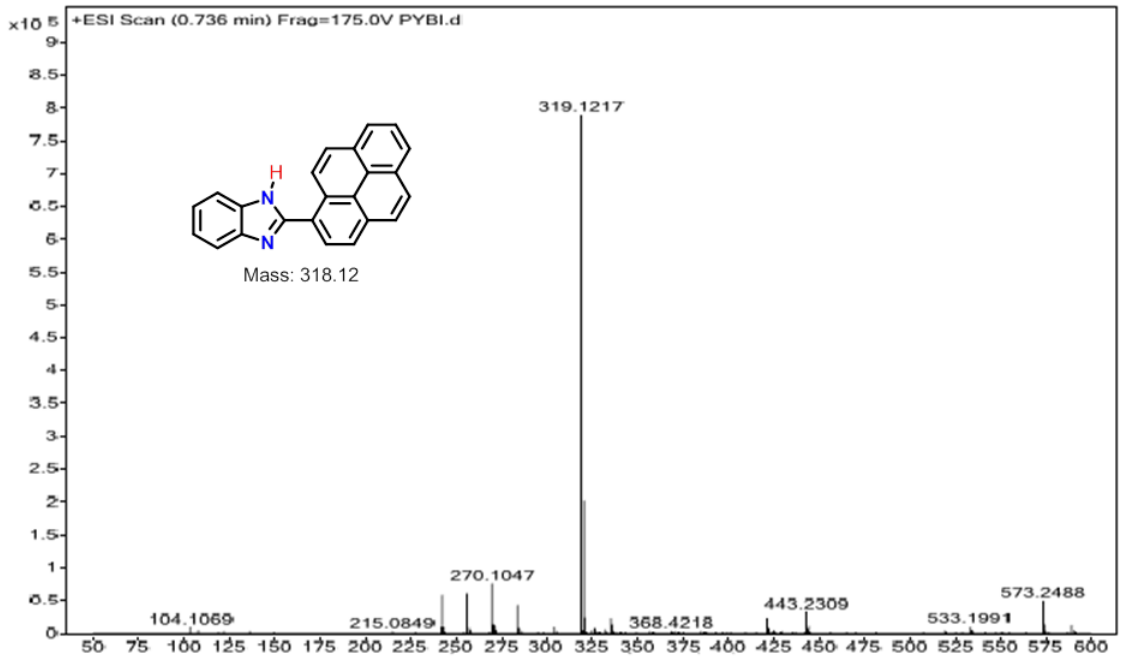

Fig. S5 High resolution mass spectrum (HRMS) of receptor **2**.

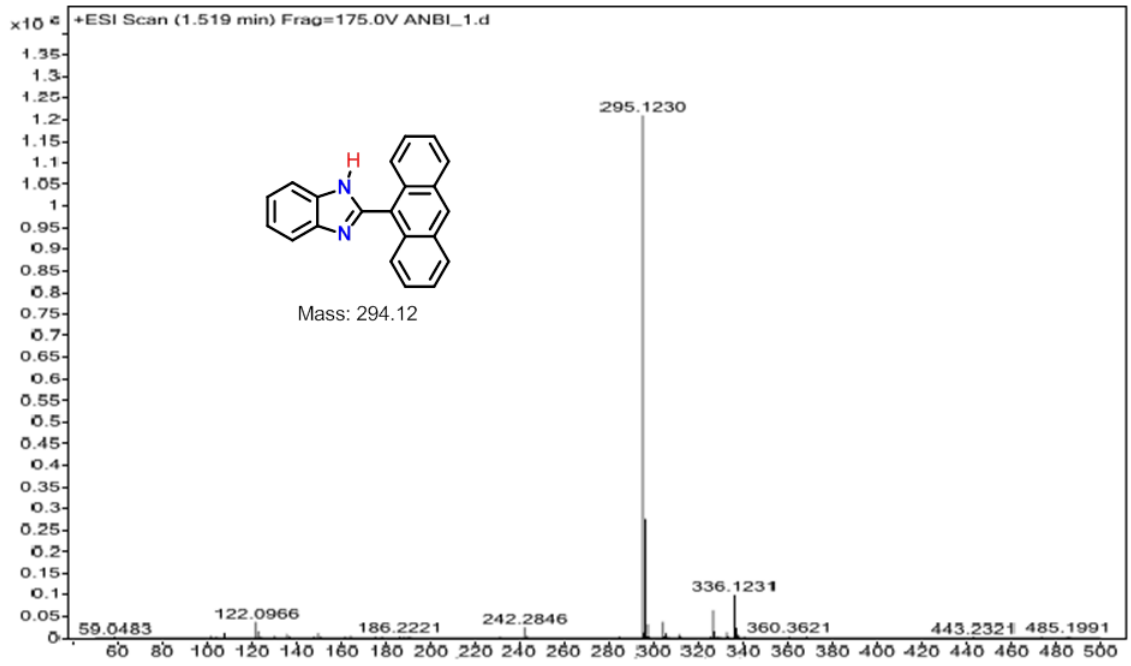

Fig. S6 High resolution mass spectrum (HRMS) of receptor **3**.

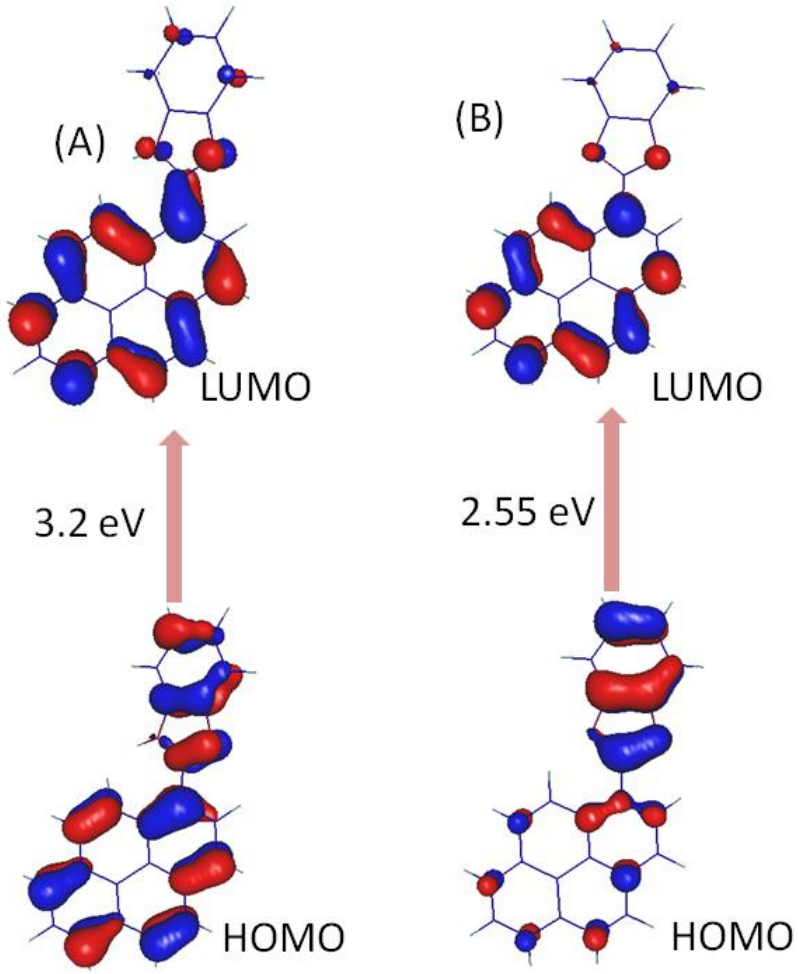

Fig. S7 HOMO-LUMO composition and transition energy of receptor **2** in neutral form (A) and in F^- induced deprotonated form (B).

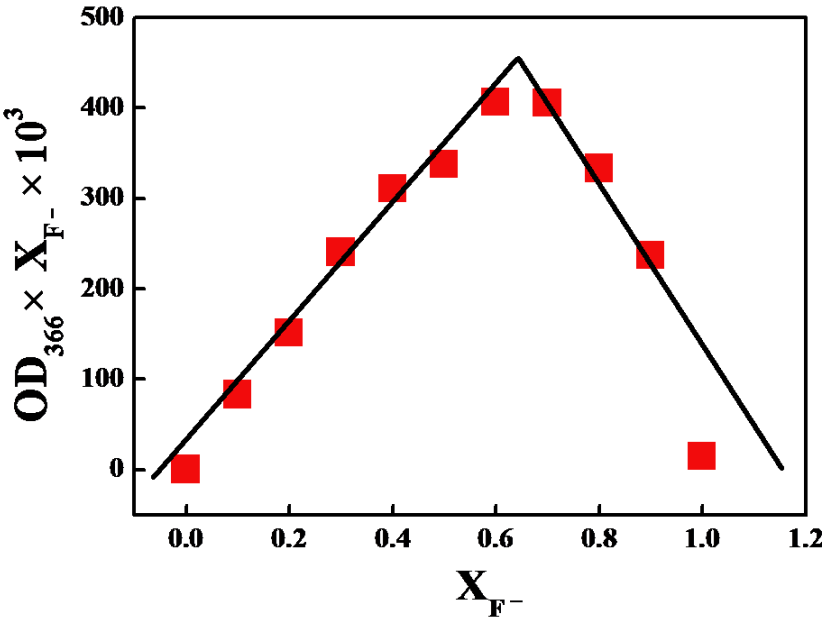

Fig. S8 Job plot for the determination of the stoichiometry of receptor **2** with F^- ions.

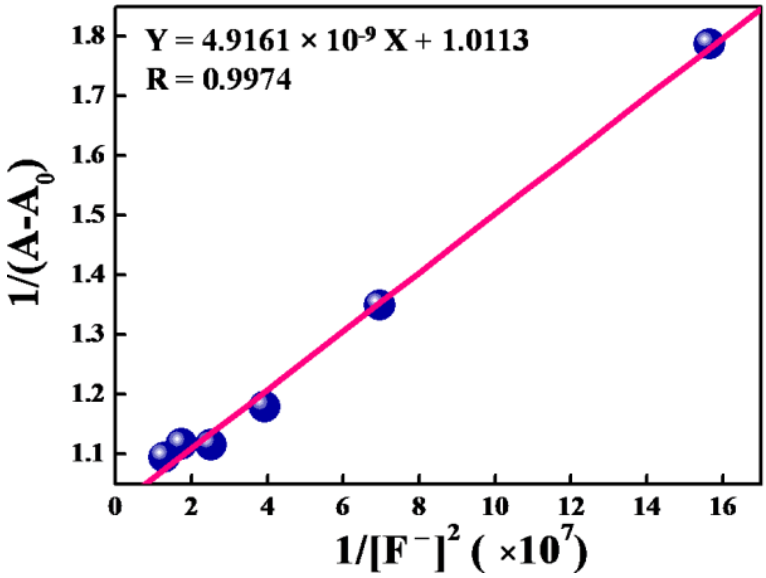

Fig. S9 Benesi-Hildebrand plot for receptor **2** with F^- ions.

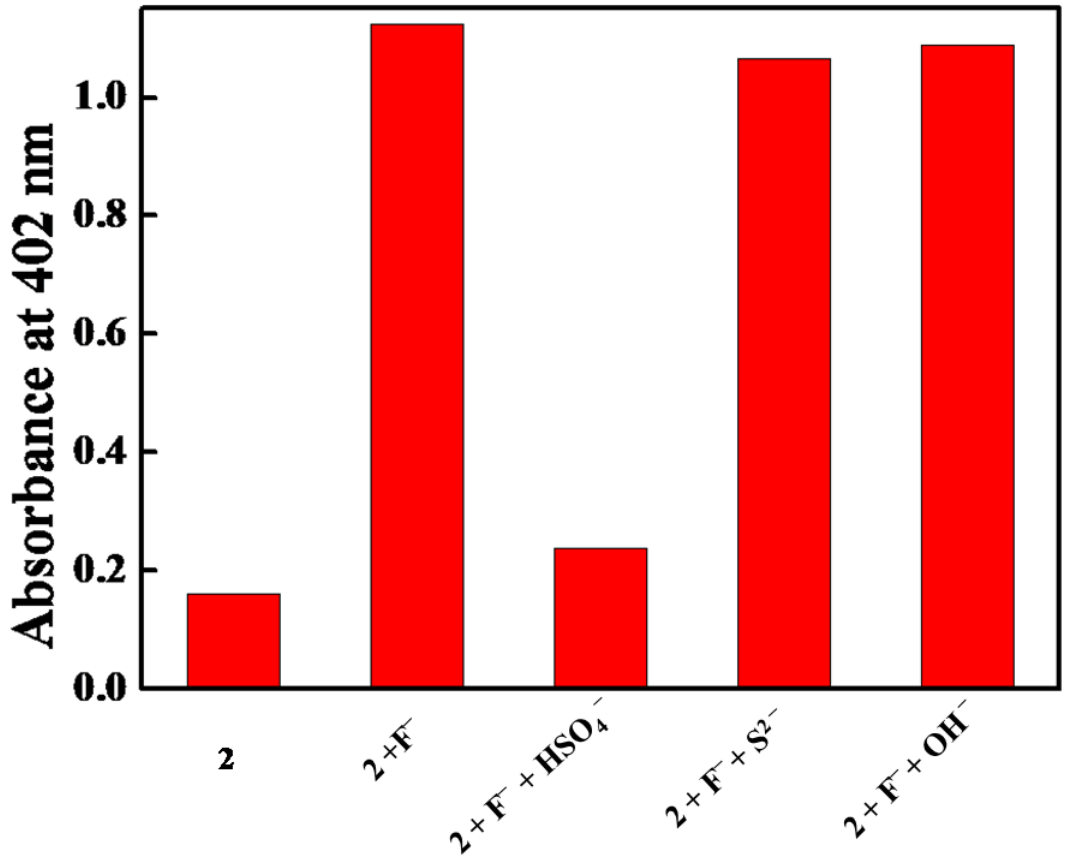

Fig. S10 Absorption spectral changes (402 nm) of competitive selectivity of 2 (2×10^{-5} M in DMSO) towards F^- (20 equiv.) in the presence of HSO_4^-, S^{2-}, OH^- ions (20 equiv.).

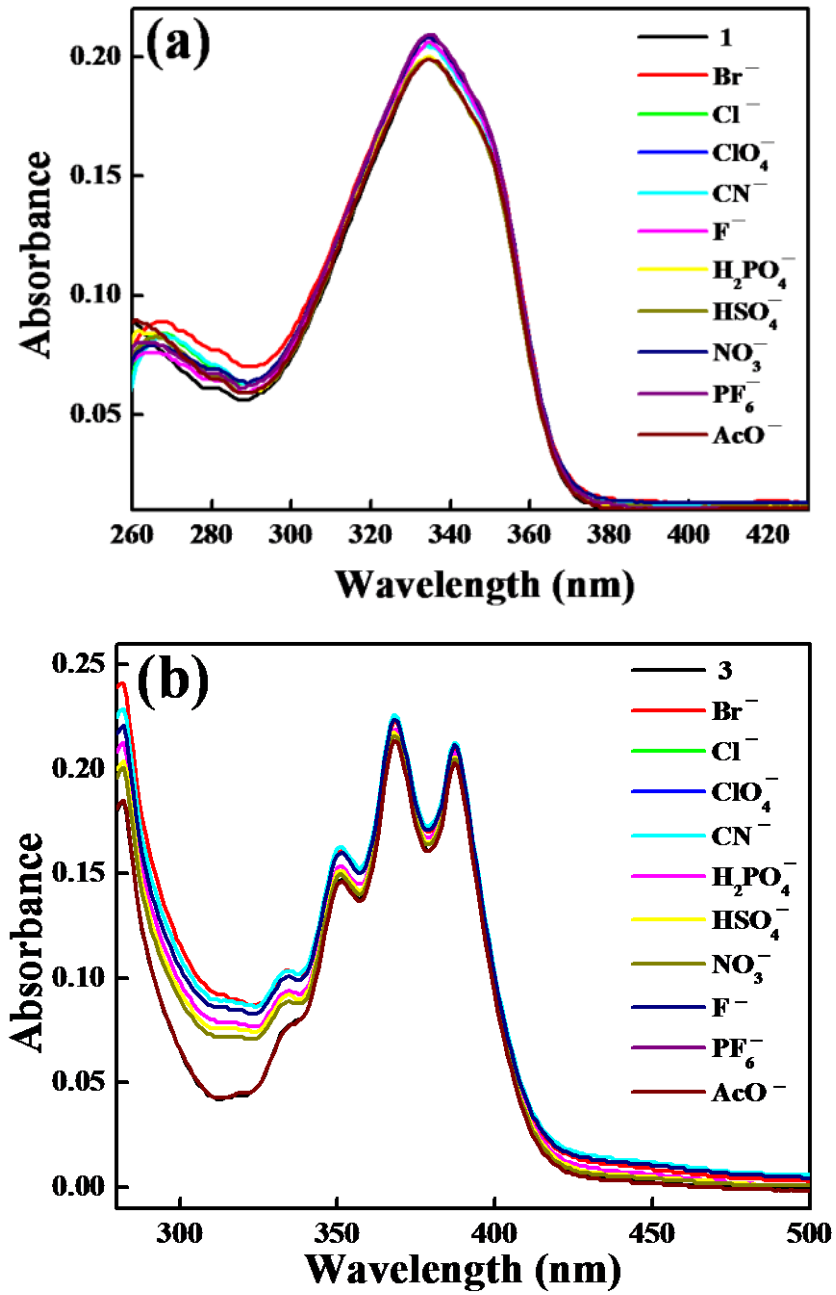

Fig. S11 Changes in UV-vis spectra of receptor **1**(a) and **3**(b) (2×10^{-5} M in DMSO) with addition of different anions as their TBA salts.

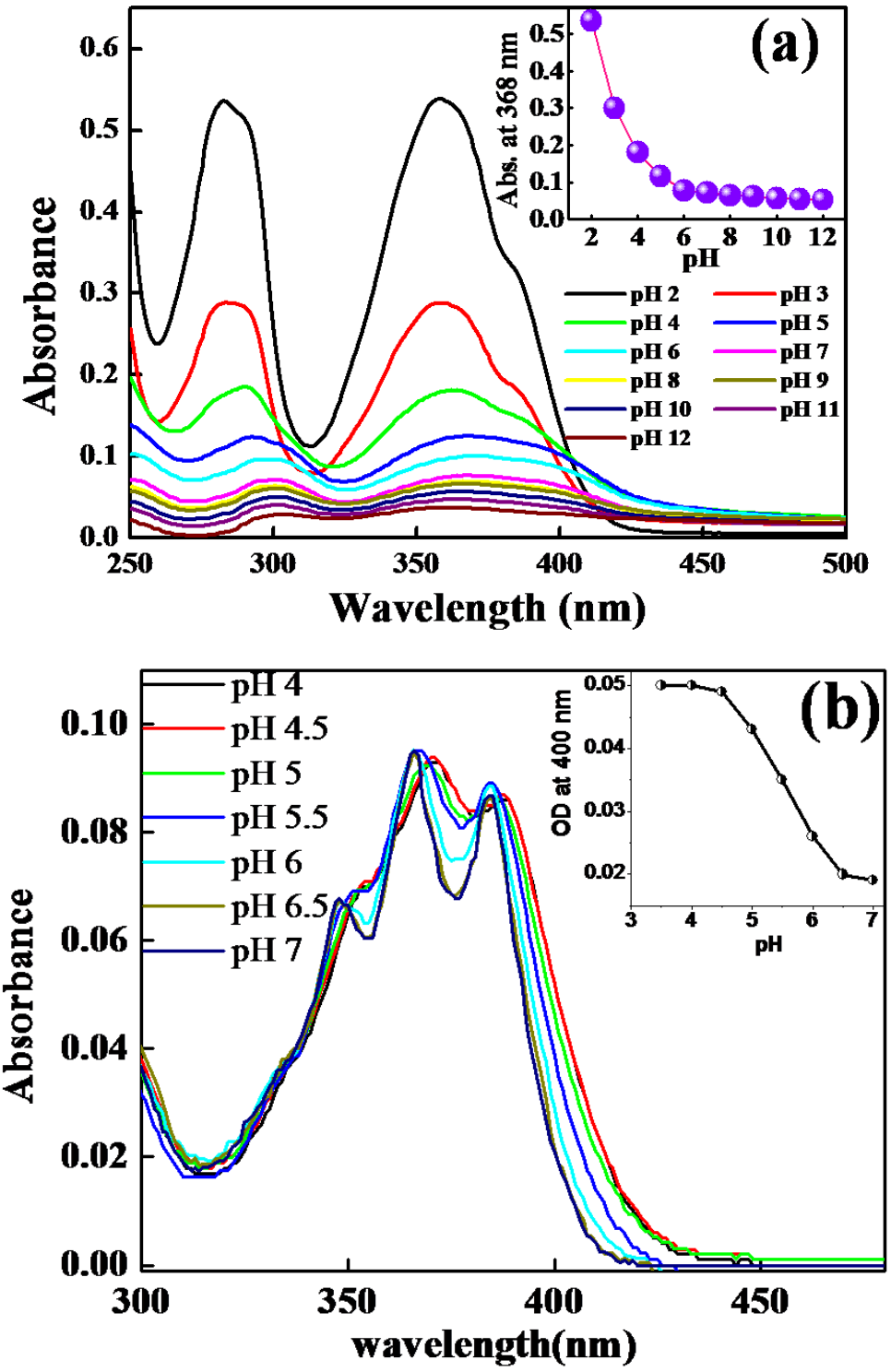

Fig. S12 Colorimetric pH titrations of receptor **2**(a) and **3**(b) in aqueous solution. Insets show the variation of absorbance at low energy peak as a function of pH which suggests p*K*a of receptor **2** and receptor **3** to be ~ 3.5 and 5-6 respectively.

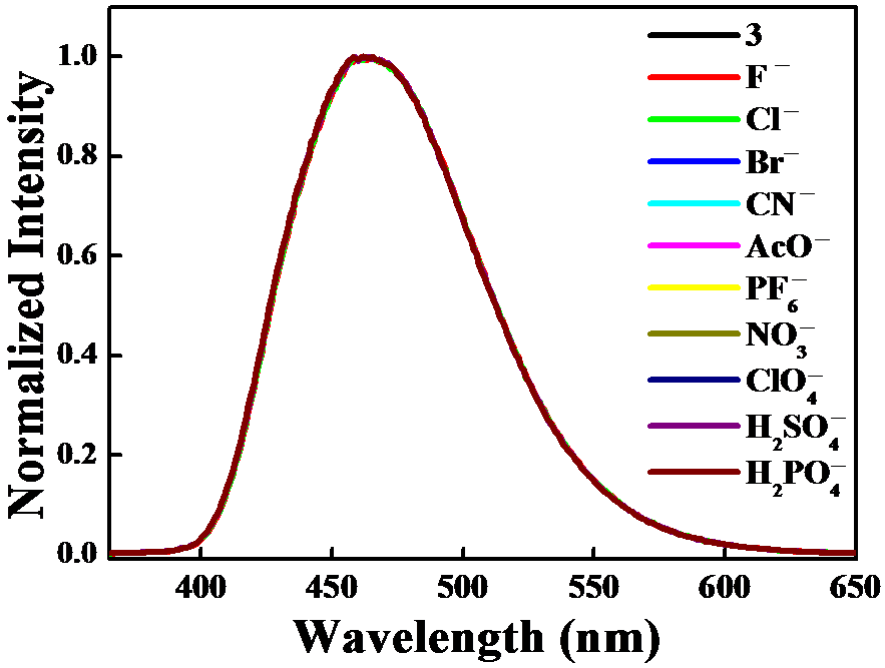

Fig. S13 Changes in emission spectra of receptor **3** (2×10^{-5} M) in DMSO with addition of different anions as their TBA salts.

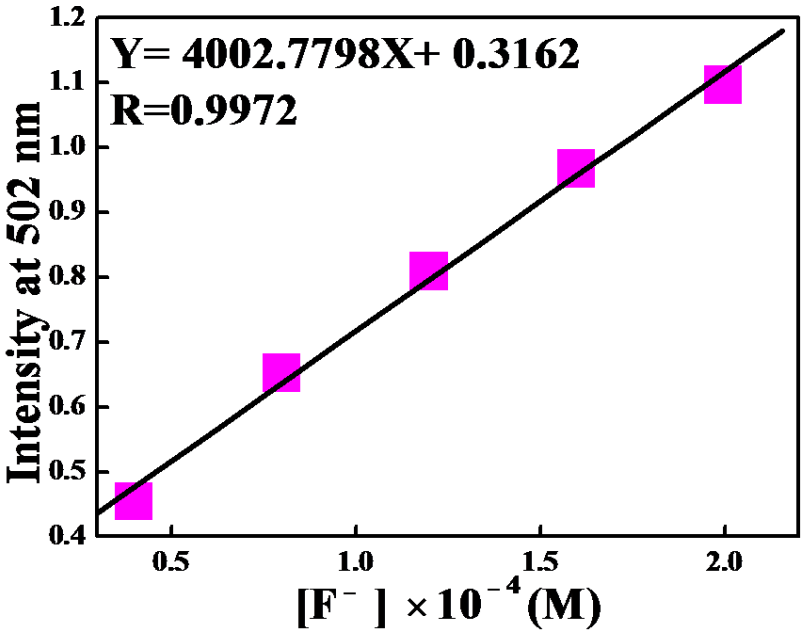

Fig. S14 Plot of emission intensity of receptor **2** at 502 nm versus concentration of F^- ions added for detection limit calculation.

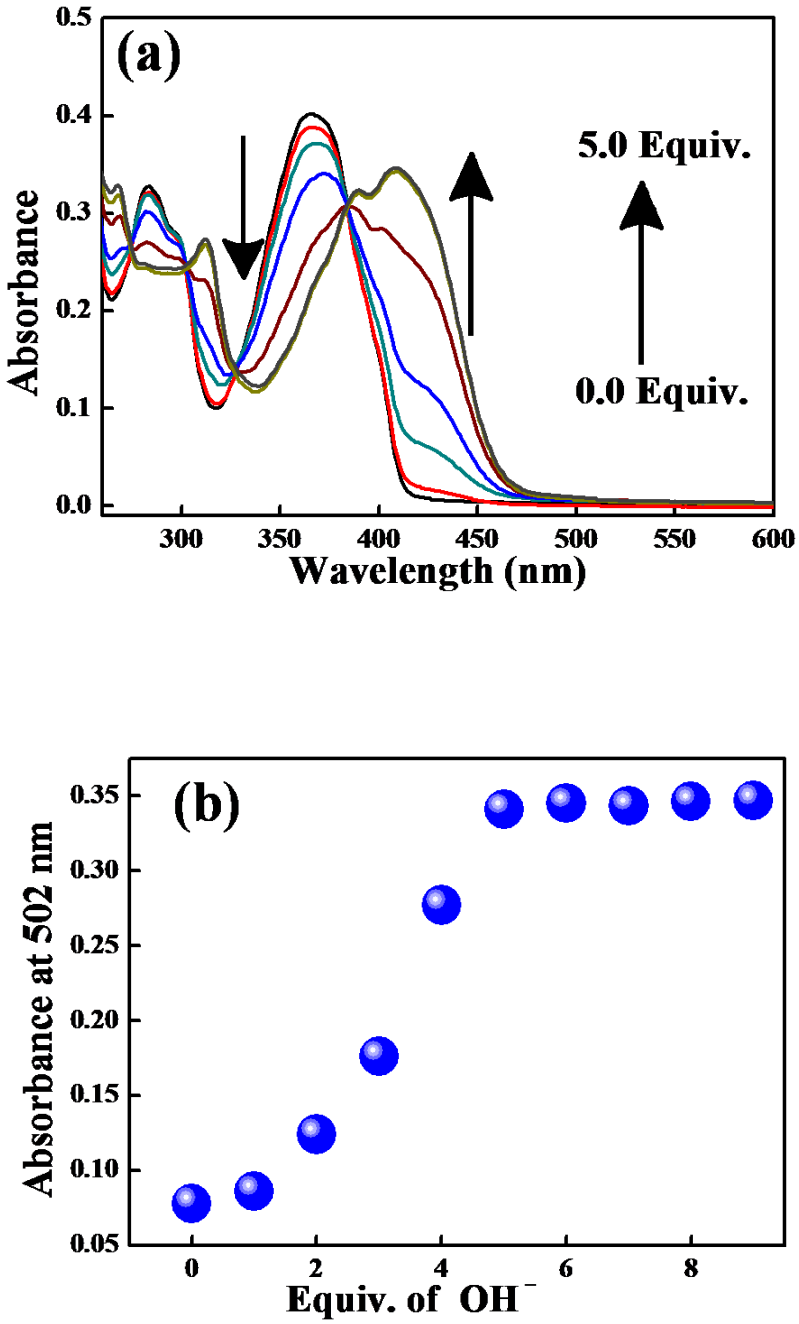

Fig. S15 Changes in absorbance of receptor **2** (2×10^{-5} M) in DMSO with addition of TBAOH.

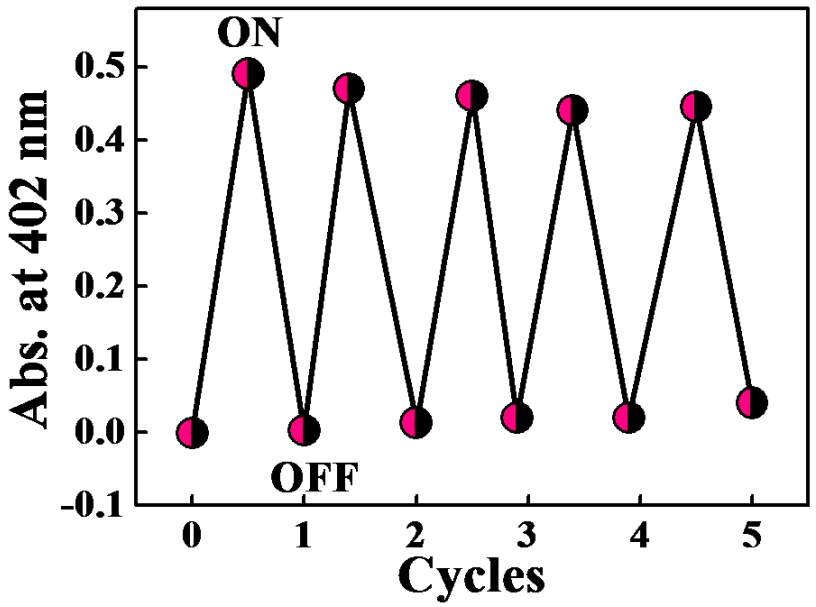

Fig.S16 Reversibility of receptor **2** with alternate addition of F^- and H^+.